Adaptive Calibration Method in Multiport Amplifier for K-Band Payload Applications

Seong-Mo Moon, Dong-Hwan Shin, Hong-yul Lee, Man-seok Uhm, In-Bok Yom, and Moon-Que Lee

This letter proposes a novel calibration method for a multiport amplifier (MPA) to achieve optimum port-to-port isolation by correcting both the amplitude and phase of the calibration signals. The proposed architecture allows for the detection of the phase error and amplitude error in each RF signal path simultaneously and can enhance the calibrated resolution by controlling the analog phase shifters and attenuators. The designed 2×2 and 4×4 MPAs show isolation characteristics of 30 dB and 27 dB over a frequency range of 19.5 GHz to 22.5 GHz, respectively.

Keywords: Multiport amplifier (MPA), phase shifter, attenuator, drive amplifier, microwave monolithic integrated circuit (MMIC), calibration, port-to-port isolation.

I. Introduction

Modern satellite communication systems generally adopt various techniques to increase the flexibility of the antenna and the power allocation of their coverage [1]. To adaptively control communication traffic during the lifetime of a satellite, using an architecture based on the multiport amplifier (MPA) is an effective approach in multibeam systems. The theoretical analysis of an MPA with respect to classical power amplification architectures reflects that it has lower DC power consumption with lower saturation power amplifiers (PAs) [2].

In this case, the isolation characteristic among the output ports of the MPA is important for successful operation. A fair port-to-port isolation characteristic can be achieved by designing Butler matrix networks and an array of PAs with minimum phase and amplitude variations. However, for practical applications, a calibration schematic should also be included in the MPA since the electrical parameters of the PAs vary with the operation environment. For satellite-based MPAs, it is necessary to minimize the number of calibration tests and reduce the complexity of on-board hardware dedicated to the MPA calibration block. Similarly, there are calibration algorithms in a smart antenna system to compensate for the antenna array errors resulting from a non-ideal feeder and the mutual coupling between radiating elements. However, the calibration algorithms are usually accomplished in a digital signal processing (DSP) domain not using the Butler matrix [3].

In previous studies on MPA calibration, all output ports were tested during calibration, as shown in Fig. 1(a). The reported calibration hardware has the following drawbacks [4], [5]: Errors are only detected through power measurements at null points (or at all output ports), and it therefore cannot be distinguished whether the cause of an error comes from an amplitude mismatch and/or a phase mismatch; The error path cannot be found among an array of signal paths. For these reasons, we propose a new calibration method for detecting the amplitude error and phase error simultaneously in each signal path [6].

A block diagram of the proposed MPA is shown in Fig. 1(b). The proposed MPA consists of an input hybrid matrix (IHM) (or a Butler matrix), amplifier modules with phase shifters (PSs) and attenuators, directional couplers, and an output hybrid matrix (OHM) in a regular sequence. The directional coupler is placed in front of the OHM to sample a signal in the path array. The calibration block for amplitude error and phase error correction consists of a modulator, a quadrature phase shift keying (QPSK) demodulator, a DSP board, and an ADC. Amplitude errors and phase errors are detected and corrected

Manuscript received Dec. 1, 2012; revised Feb. 2, 2013; accepted Feb. 12, 2013.

Seong-Mo Moon (phone: +82 42 860 0862, smmoon@etri.re.kr), Dong-Hwan Shin (dhshin@etri.re.kr), Hong-yul Lee (hylees@etri.re.kr), Man-seok Uhm (msuhm@etri.re.kr), and In-Bok Yom (ibyom@etri.re.kr) are with the Broadcasting & Telecommunications Media Research Laboratory, ETRI, Daejeon, Rep. of Korea.

Moon-Que Lee (corresponding author, mqlee@uos.ac.kr) is with the School of Electrical and Computer Engineering, University of Seoul, Seoul, Rep. of Korea.

http://dx.doi.org/10.4218/etrij.13.0212.0534

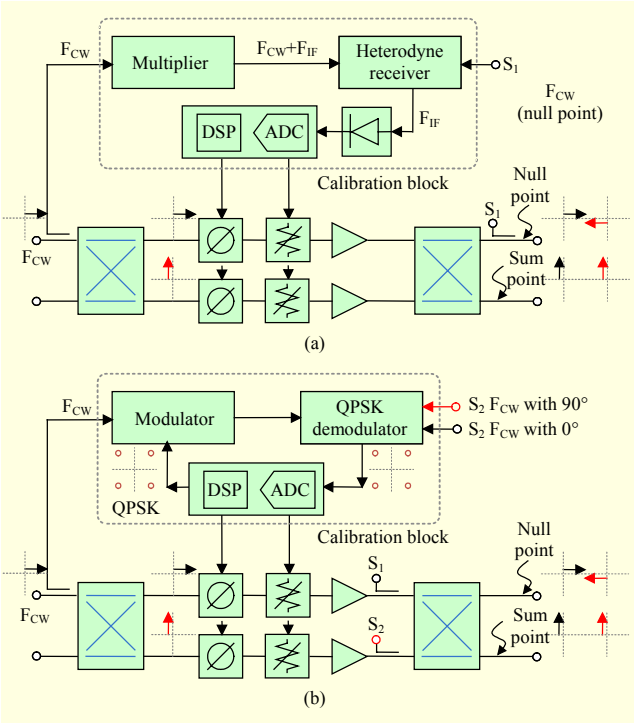

Fig. 1. Functional block diagrams of (a) conventional and (b) proposed 2×2 MPAs with calibration block.

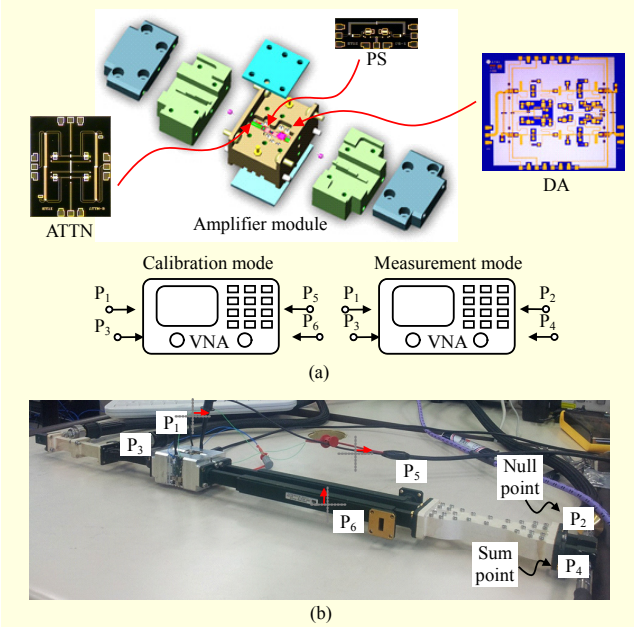

Fig. 2. (a) 3D image of amplifier module and designed MMICs and (b) photograph of proposed 2×2 MPA and measurement set-up.

through a calculation of the axial ratio in the calibration block. The proposed architecture of the MPA allows for the detection of both the amplitude and phase of each output port, whereas the conventional architecture shown in Fig. 1(a) allows for the detection of only the amplitude. Due to this difference, the proposed MPA is faster and has less iterations.

II. Design and Implementation

The amplifier module shown in Fig. 2(a) includes three in-house designed monolithic microwave integrated circuits (MMICs): an analog PS, a voltage variable attenuator (ATTN), and a drive amplifier (DA). The MMICs are fabricated through a 0.15-μm GaAs HEMT process. The amplitude variation of the PS is below 0.4 dB within a 90-degree phase-shift range, and the phase variation of the ATTN is below 4 degrees during a 7-dB attenuation operation. The directional couplers are constructed with a WR-42 interface and have a 12-dB coupling factor. The 2×2 MPA is implemented in the form of a waveguide assembly composed of 3-dB branch-line couplers, amplifier modules, and directional couplers for sampling a signal, as shown in Fig. 2(b). Planar-type 3-dB couplers with a waveguide interface are constructed.

For simple verification of the proposed MPA calibration algorithm described in this letter, we use a vector network analyzer (VNA) before implementing the calibration hardware, as shown in Fig. 2(b). In calibration mode, a four-port VNA is used to measure all *S*-parameters between the input ports and each coupled port to detect the amplitude error and phase error, which are then compared with the amplitude and phase characteristics of an ideal MPA. Finally, the amplitude error and phase error are corrected manually by controlling the ATTN and PS in the amplifier module.

Figure 3 shows a block diagram and photograph of the 4×4 MPA implemented in the form of a waveguide assembly composed of two 4×4 hybrid matrices, amplifier modules, and directional couplers. The 3D image and measured data of the proposed planar 4×4 hybrid matrix are shown in Fig 4. The proposed 4×4 hybrid matrix consists of three 0-dB cross couplers and four 3-dB couplers connected by E-plane bended waveguides. A 3-dB branch-line coupler is designed with six slots with a 1:3:4:4:3:1 voltage coupled ratio to achieve a wide bandwidth of more than 3 GHz. One 0-dB cross coupler is implemented by two 3-dB couplers in a cascade connection to overcome the crossing problem and obtain wideband performances. To achieve the same phase with the crossing line, another 0-dB cross coupler is placed in a straight line. For the signal injected into Port 1 (P_1), which is the input port, the insertion loss, return loss, and isolations are measured as below 0.2 dB, above 30 dB, and above 30 dB, respectively, as shown in Fig. 4. The maximum output magnitude imbalance and phase imbalance are 0.7 dB and 2 degrees over the frequency range of 19.5 GHz to 22.5 GHz, respectively.

The isolation characteristics among the output ports are

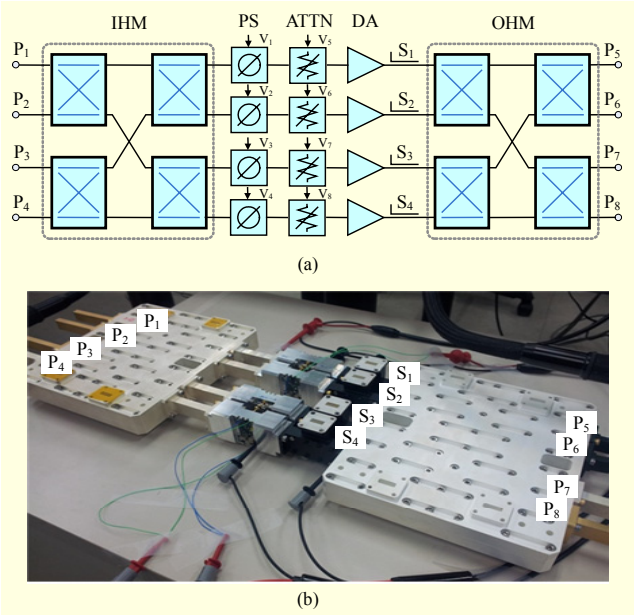

Fig. 3. (a) Block diagram and (b) photograph of proposed 4×4 MPA and test set-up.

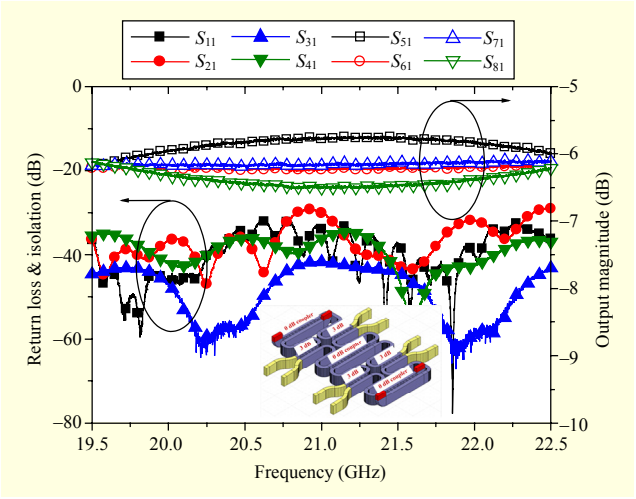

Fig. 4. Measured data and 3D image of 4×4 hybrid matrix.

important for a successful operation. To obtain excellent isolation characteristics, it is necessary to design and construct the MPA with a minimum number of phase errors and amplitude errors.

III. Verification of Calibration Method

Figure 5 shows the phase and amplitude characteristics of each coupled port in the proposed 2×2 MPA, which are marked as Port 5 (P_5) and Port 6 (P_6) in Fig. 2(b), respectively. The black lines (the dotted line represents before calibration, and the solid line represents after calibration) show the output

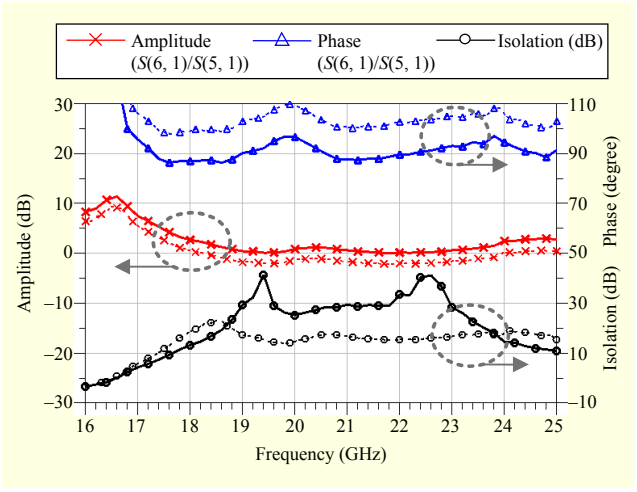

Fig. 5. Measured phase error and amplitude error of proposed 2×2 MPA shown in Fig. 2(b).

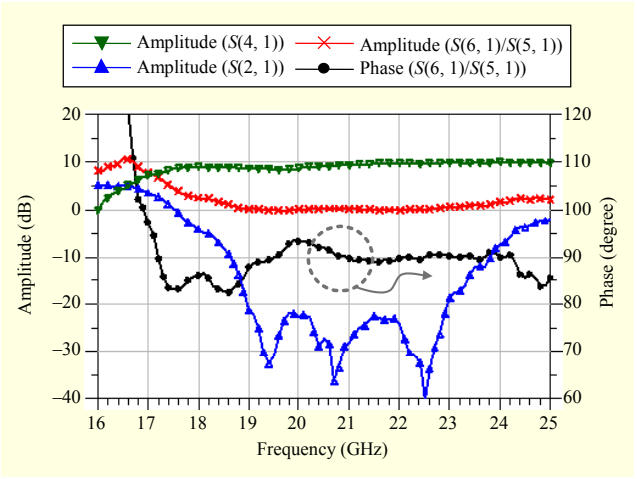

Fig. 6. Measured *S*-parameters of proposed 2×2 MPA shown in Fig. 2(b).

port-to-port isolation characteristics. The isolation characteristics are improved by 10 dB after the calibration within the operation frequency band of 19.5 GHz to 22.5 GHz. The blue and red lines respectively show the measured relative phase variation and amplitude variation, before (dotted line) and after (solid line) the calibration, in two coupled ports. After the calibration, the relative phase error and amplitude error between Ports 5 and 6 are 92 degrees ± 5 degrees and less than 0.5 dB from 19.5 GHz to 22.5 GHz, respectively. Figure 6 shows the measured results of the proposed 2×2 MPA. The return losses in all ports are measured as greater than 30 dB over the frequency range of 19.5 GHz to 22.5 GHz. The port-to-port isolation characteristic is greater than 30 dB.

Figure 7 shows the port-to-port isolation of the realized 4×4 MPA for a continuous wave signal injected into Port 1 (P_1). After the identical calibration process of the 2×2 MPA, the

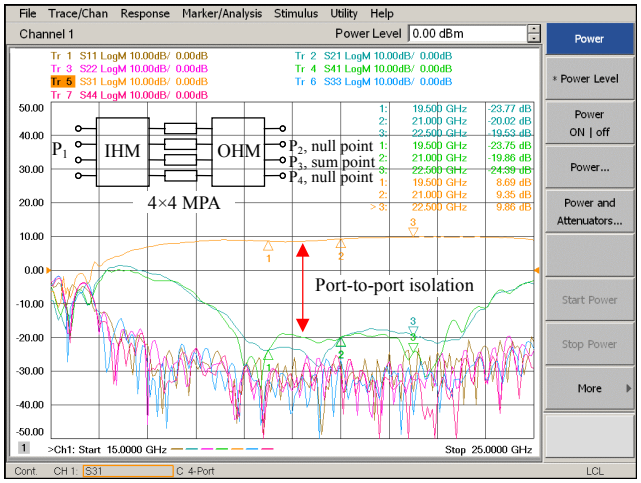

Fig. 7. Measured *S*-parameters of proposed 4×4 MPA.

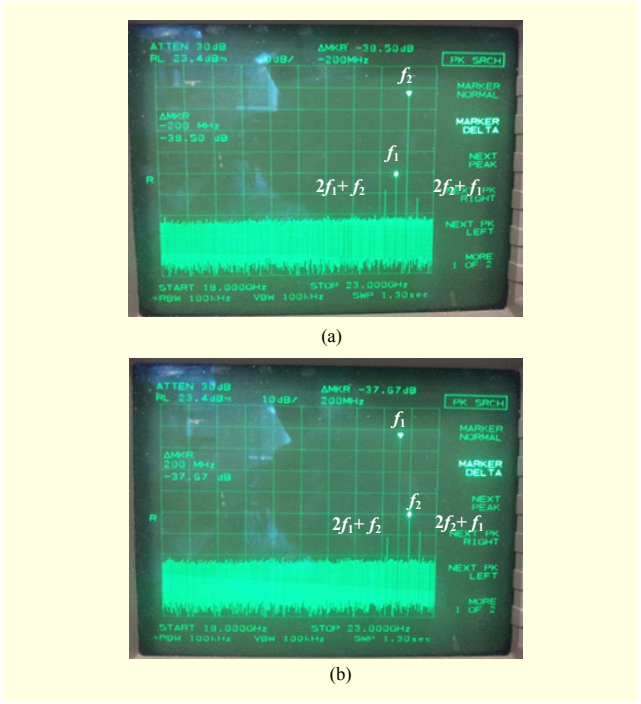

Fig. 8. Output power spectrum at Ports 8 and 5 when two signals are applied to Ports 1 and 4, simultaneously.

isolation characteristic is measured as above 27 dB over the measured frequency band.

To evaluate the intermodulation characteristics of an MPA, two signals, f_1 and f_2, with a frequency offset of 200 MHz are applied to Ports 1 and 4, respectively. The input power level of each amplifier is 10 dBm. Figure 8 shows the output power spectrum at the corresponding output ports, Ports 8 and 5. At Port 5, an output signal with carrier frequency f_1, an unwanted frequency f_2, and third-order intermodulation products $2f_2–f_1$ and $2f_1–f_2$ are measured. The isolation and intermodulation products are measured as 30 dB and –45 dBc, respectively.

Table 1. Performance comparison of [7] with this work.

Parameter	[7]	This work	
	8×8	2×2	4×4
Frequency (GHz)	17.7 to 18.7	19.5 to 22.5	
Port-to-port isolation (dB)	> 25	> 30	>27
Input/output return loss (dB)	NA	>27	
Attenuation range (dB)	3	7	
PS range (degree)	45	90	

Table 1 shows a comparison of the main characteristics of the previously reported MPA [7] and those of the proposed MPA.

IV. Conclusion

A novel calibration method based on analog-controlled error compensation was applied to 2×2 and 4×4 MPAs and showed excellent port-to-port isolation of over 30 dB and 27 dB over a wide frequency range of 19.5 GHz to 22.5 GHz, respectively. The proposed calibration directly detects sampling signals in the path array, whereas the systems presented in previous works detect the output signals at the null point. Comparatively, the proposed MPA is straightforward and has low complexity.

References

[1] U. Park et al., "A Dynamic Bandwidth Allocation Scheme for a Multi-spot-beam Satellite System," *ETRI J.*, vol. 34, no. 4, Aug. 2012, pp. 613-616.

[2] A. Mallet et al., "Multiport-Amplifier-Based Architecture versus Classical Architecture for Space Telecommunication Payloads," *IEEE Trans. MTT*, vol. 54, no. 12, Dec. 2006, pp. 4353-4361.

[3] D.H. Lee and C.S. Pyo, "RF Performance and Effect of Calibration in Smart Antenna System," *IEEE 59th Veh. Technol. Conf.*, 2004, pp. 30-33.

[4] X. Huang and M. Caron, "Self-Calibrating Multi-port Circuit and Method," Patent applications filed in Canada, USA, and Europe, US 2008/0143562 Al.

[5] Z. Zhu, X. Huang, and M. Caron, "Ka-Band Multi-port Power Amplifier Calibration Experiment and Results," *2nd Int. Conf. Adv. Satellite Space Commun.*, 2010, pp. 11-14.

[6] S. Moon et al., "Adaptive Amplitude and Phase Calibration of Multi-port Amplifier Using Modified Six-Port Demodulator," *Proc. 17th Ka Broadband Commun. Conf.*, 2011.

[7] I. Hosoda et al., "Ka Band High Power Multi-port Amplifier (MPA) Configured with TWTA for WINDS Satellite," *IEEE Int. Vacuum Electron. Conf.*, 2007, pp. 401-402.